Backscattering from Resistive Strips

by

Thomas B. A. Senior
Radiation Laboratory, The University of Michigan
Ann Arbor, Michigan 48109

Abstract

Strips made of a resistive sheet material have lower backscattering cross sections than the corresponding perfectly conducting strips, and this is true in particular when the illumination is edge-on with the electric vector parallel to the edge. Attention is focused on this case. Using the moment method applied to an appropriate integral equation, data are obtained for the surface field and backscattered far field of a resistive strip for a variety of strip widths w and uniform resistances R. The front and rear edge contributions to the far field are then extracted. It is shown that for strips whose width is greater than about a half wavelength the former is the same as for a half plane having the same resistance, whereas the latter is proportional to the square of the current at that point on the half plane corresponding to the rear edge of the strip. The implications of these results on the selection of a strip resistance for low backscattering are discussed.

1. Introduction

The backscattering properties of perfectly conducting strips or ribbons have been extensively explored both analytically and numerically and the strip is widely used as a model in scattering investigations. From the eigenfunction expansion in terms of Mathieu functions data have been obtained for strips up to a wavelength or two in width, and asymptotic expansions have been developed which accurately predict the scattering for strips as narrow as a half wavelength. Not surprisingly, the backscattering decreases at angles away from broadside and is, in fact, zero at grazing incidence when the magnetic vector is parallel to the edge (H polarization). For E polarization, however, the edge-on backscattering is non-zero, and when the strip is regarded as a model, for example, of an aircraft wing or tail fin, the scattering can be large enough to be significant. The desire to reduce the scattering in this case leads naturally to a consideration of non-metallic strips.

For this purpose a strip made of a resistive sheet material is attractive because, like a perfectly conducting strip, it is invisible to an H-polarized plane wave at grazing incidence. During the last few years the concept of a resistive sheet has found several applications. To see how this comes about, consider a thin sheet of highly conducting material whose permeability is that of free space. If σ is the conductivity and τ is the thickness of the sheet, we can define a surface resistance R as $R = (\sigma\tau)^{-1}$ ohms, and as $\tau \to 0$ we can imagine σ to increase in such a manner that R is finite in the limit. The result is an infinitesimally thin sheet whose electromagnetic properties are specified by the single measurable quantity R. Though this is obviously an idealization, it is not difficult to fabricate a sheet no more than 0.1 mm in thickness and presenting an almost constant resistance as large as 1800 ohms over a wide range of frequencies, with the precise value depending on the amount of carbon loading employed.

In this paper we consider the scattering properties of uniform resistive strips of finite width illuminated by a plane electromagnetic wave incident in a plane perpendicular to the edge with electric vector parallel to the edge. Our primary concern is backscattering at grazing incidence and its dependence on the resistance and strip width. From an examination of the known analytical solution [1] for a resistive half plane, the current on the infinite structure is computed and the backscatter-

ing attributable to the edge determined. For strips of various resistances and finite widths, the induced currents and backscattering cross sections are obtained by numerical solution of the appropriate integral equation. The currents are remarkably similar to those on a half plane and from the backscattering data the front and rear edge contributions are extracted. The former is the same as for a half plane and the latter is proportional to the square of the current amplitude at that position on a half plane corresponding to the rear edge of the strip. Factors affecting the choice of a strip resistance for low backscattering are briefly discussed.

2. Formulation

Consider a strip of width w and resistance R occupying the portion $0 \le x \le w$, $-\infty < z < \infty$ of the plane $y = 0$ of a cartesian coordinate system (x,y,z). The strip is illuminated by an E-polarized plane electromagnetic wave

$$\underline{E}^i = \hat{z}\, e^{-ik(x\cos\phi_0 + y\sin\phi_0)} \tag{1}$$

(see Fig. 1) where $0 \le \theta_0 \le \pi$ and a time factor $e^{-i\omega t}$ has been suppressed. Since the total electric field also has only a z component, the conditions at the surface of the strip can be written as

$$E_z(x,0+) = E_z(x,0-) = RJ$$

with

$$J = -[H_x]^+_-$$

being the total z-directed current induced in the strip. We remark that when $R = 0$ the strip is perfectly conducting, and when $R = \infty$ it no longer exists.

The scattered electric field is

$$E_z^s = -\frac{kZ}{4} \int_0^w J(x') H_0^{(1)}(k\sqrt{(x-x')^2 + y^2})\, dx' \tag{2}$$

where $H_0^{(1)}$ is the cylindrical Hankel function of the first kind of order zero and Z is the intrinsic impedance of free space. In the far zone,

$$E_z^s \sim \sqrt{\frac{2}{\pi k\rho}}\, e^{i(k\rho - \pi/4)} P(\phi,\phi_0)$$

where (ρ,ϕ) are cylindrical polar coordinates such that $x = \rho\cos\phi$ and

$y = \rho\sin\phi$, and the complex scattering amplitude P is

$$P(\phi,\phi_0) = \frac{-kZ}{4}\int_0^w J(x')\, e^{ikx'\cos\phi} dx' \ .$$

In terms of P the two dimensional scattering cross section (or length) is

$$\sigma(\phi,\phi_0) = \frac{2\lambda}{\pi}\,|P(\phi,\phi_0)|^2 . \qquad (3)$$

For edge-on incidence ($\phi_0 = \pi$) the front edge of the strip is the one coincident with the z axis.

From (1) and (2), on allowing the observation point to lie on the strip and then applying the boundary condition, the following integral equation results:

$$RJ(x) = e^{-ikx\cos\phi_0} - \frac{kZ}{4}\int_0^w J(x')H_0^{(1)}(k|x-x'|)dx' \qquad (4)$$

for $0 < x < w$. A computer program has been written to solve this by the moment method and thence compute the backscattered far field, and this was used to generate the data to be presented later.

3. Half Plane

In the particular case of a half plane ($w=\infty$) the integral equation (4) is of the Wiener-Hopf type and can be solved analytically. As shown in [1,2]

$$ZJ(x) = \frac{-i}{\pi}\int_C \frac{1}{\zeta+k\cos\phi_0}\ \frac{\sqrt{k^2-\zeta^2}}{k+\eta\sqrt{k^2-\zeta^2}}\ \frac{K_+(-k\cos\phi_0)}{K_+(\zeta)}\, e^{i\zeta x}\, d\zeta$$

where $\eta = 2R/Z$, $K_+(\zeta)$ is a 'split' function analytic and free of zeros in the upper half ζ plane, and the path C runs from $-\infty$ to ∞ with indentations above the branch point at $\zeta=-k$ but below the pole at $\zeta=-k\cos\phi_0$ and the branch point at $\zeta=k$ (see Fig. 2). For edge-on incidence the latter branch point and the pole coalesce, giving

$$ZJ(x) = \frac{-i}{\pi}\int_C \frac{1}{\zeta-k}\ \frac{\sqrt{k^2-\zeta^2}}{k+\eta\sqrt{k^2-\zeta^2}}\ \frac{K_+(k)}{K_+(\zeta)}\, e^{i\zeta x}\, d\zeta \qquad (5)$$

and throughout the remainder of this section we shall confine attention to the case $\phi_0=\pi$.

If the half plane is perfectly conducting ($\eta=0$)

$$K_+(\zeta) = \sqrt{\frac{k+\zeta}{k}} \qquad (6)$$

and the integral in (10) can be evaluated analytically to give

$$ZJ(x) = 2\sqrt{\frac{2}{\pi kx}}\, e^{i(kx+\pi/4)} \tag{7}$$

which is infinite at the edge. If $\eta \neq 0$ the behavior of the current far from the edge is specified by the nature of the singularity of the integrand at $\zeta=k$, closest to the origin of the ζ plane. From this we have

$$ZJ(x) \sim 2\sqrt{\frac{2}{\pi kx}}\, e^{i(kx+\pi/4)} \tag{8}$$

as $kx \to \infty$, showing that the current on a resistive half plane asymptotically approaches that on a perfectly conducting half plane at large distances from the edge. The behavior close to the edge is determined by the order of the integrand for large $|\zeta|$, and since $K_+(\zeta) \sim \eta^{-1/2}$ as $|\zeta| \to \infty$, it follows that

$$ZJ(0) = 2\eta^{-1/2} K_+(k) . \tag{9}$$

$K_+(k)$ has been computed [1] and Fig. 3 shows a plot of $ZJ(0)$ for $0.1 \leq \eta \leq 10$. In addition, asymptotic approximations [1] to $K_+(k)$ give

$$ZJ(0) \simeq \begin{cases} 2\left(\frac{2}{\eta}\right)^{1/2} \exp\left\{-\frac{\eta}{\pi}\left(1-\ell n\frac{\eta}{2}\right)\right\} & |\eta| \ll 1 \\ \frac{2}{\eta} \exp\left(-\frac{1}{\pi\eta}\right) & |\eta| \gg 1 \end{cases} \tag{10}$$

and the curves corresponding to these expressions are included in Fig. 3. They cover the entire range of η with surprising accuracy, and even for $\eta=1$ the small and large resistance approximations differ by only 20 percent and are individually in error by no more than 10 percent. Such accuracy is adequate for many practical purposes, and the formulas (10) are valid for complex η as well as real.

To find the current away from the edge but at distances less than those for which (8) is applicable, the obvious approach is to compute the integral in (5). Unfortunately, attempts to do this numerically using an integral expression for the split function ratio have proved unsuccessful, and as an alternative we shall use data computed from (4) for strips of large width w. It is found that as w increases, the current over a distance of (say) 3λ from the front edge becomes less and less dependent on the strip width and, for $w \gtrsim 6\lambda$, can be treated as the current on the corresponding portion of a half plane. The result-

ing half plane currents for different η are shown in Fig. 4, and we observe that for fixed x the amplitude decreases with increasing η.

The scattered field for edge-on incidence can be obtained by substituting (5) into (2) and using the Fourier integral representation of the Hankel function. Thus

$$E_z^s(\rho,\phi) = -\frac{k}{2\pi i}\int_C \frac{1}{\zeta-k}\,\frac{1}{k+\eta\sqrt{k^2-\zeta^2}}\,\frac{K_+(k)}{K_+(\zeta)}\,e^{i\rho(\zeta\cos\phi+\sqrt{k^2-\zeta^2}|\sin\phi|)}\,d\zeta$$

and for $\phi=\pi$ a stationary phase evaluation yields the following expression for the far field amplitude:

$$P(\pi,\pi) = \frac{-i}{4}\{K_+(k)\}^2 . \qquad (11)$$

In the particular case of a perfectly conducting half plane we have $K_+(K)=\sqrt{2}$, giving $P(\pi,\pi) = -i/2$, and the ratio of (11) to its perfectly conducting value is plotted as a function of η, $10^{-2} \le \eta \le 10^2$, in Figure 1 of [1]. The ratio decreases monotonically from unity for $\eta=0$ to zero for $\eta=\infty$.

4. Finite Width Strips

Using the moment method the integral equation (4) has been solved for a variety of resistances $R(=\eta Z/2)$ and strip widths $w\le 6\lambda$. The sampling rate was never less than 16 points per wavelength, and since no interpolation formula was employed, the rate was increased in the immediate vicinity of the front edge, reaching a maximum of 2000 points per wavelength for a perfectly conducting strip whose current is infinite at the edge. We again concentrate on the case of edge-on incidence.

For a perfectly conducting strip of width $w\gtrsim\lambda/2$ the current is almost identical to that on the corresponding portion of a half plane. This is illustrated in Fig. 5, where the current amplitude on a strip of width 3λ is compared with that given by (7), and the only noticeable differences are within about $\lambda/2$ of the rear edge. The edge-on backscattering cross section σ/λ is plotted as a function of w/λ in Fig. 6. The rather regular oscillation with minima $\lambda/2$ apart is suggestive of an interference between front and rear edge contributions, and according to the asymptotic expansion of Fialkovskiy [3],

$$P(\pi,\pi) \sim -\frac{i}{2} - \frac{e^{2ikw}}{4\pi kw} \qquad (12)$$

for large kw, implying

$$\frac{\sigma}{\lambda} \simeq \frac{1}{2\pi}\left\{1 + \frac{\sin 2kw}{\pi kw} + \frac{1}{(2\pi kw)^2}\right\}. \tag{13}$$

The resulting curve is included in Fig. 6, and we observe that the approximation is good for all $w \geq \lambda/2$.

From (12) the front edge contribution is clearly -i/2 and is identical to that for a half plane. The rear edge contribution is therefore

$$P^r(\pi,\pi) = -\frac{e^{2ikw}}{4\pi kw} \tag{14}$$

and we note that if J(w) is the half plane current measured at a distance w from the edge,

$$P^r(\pi,\pi) = \frac{i}{32}\{ZJ(w)\}^2. \tag{15}$$

The relationship is analogous to that for a traveling wave [4] in the case of H polarization.

For resistive strips having $\eta \neq 0$ the currents are also similar to those on the corresponding half planes, and this can be seen from Fig. 7 where the current amplitudes on strips of width $w=3\lambda$ having $\eta=1$, 4 and 10 are compared with the half plane currents shown in Fig. 4. The strip currents oscillate about the half plane values, but the oscillations, indicative of a reflected contribution, are small except close to the rear edge and decrease with increasing distance from the rear.

The backscattering cross sections of strips having $\eta=1$, 4 and 10 are plotted as functions of the strip width w, $0 \leq w \leq 3\lambda$, in Fig. 8. As in the case of Fig. 6, the regular oscillations with minima $\lambda/2$ apart suggest an interference between front and rear edge contributions. To determine their individual values, an expression for the far field amplitude of the form

$$P(\pi,\pi) = P^f(\pi,\pi) + e^{2ikw}\{e^{-2ikw}P^r(\pi,\pi)\} \tag{16}$$

was assumed, with P^f independent of w and $e^{-2ikw}P^r$ at most a slowly varying function. We then sought the best fit to the computed data for $|P|$ and arg P. For a few values of η, the resulting front edge contributions are listed in Table 1, and are almost identical to those for the corresponding half planes. For these same η, the amplitudes of the rear edge contributions as functions of w are shown in Fig. 9.

Apart from some slight oscillations for $w \lesssim \lambda/2$, the amplitudes decrease uniformly with increasing w from the value $2\eta^{-1/2}K_+(k)$ of (9) for strips of vanishing width. We also remark that

$$\arg P^r(\pi,\pi) = 2kw + \Phi(w)$$

where, for increasing w, $\Phi(w)$ increases from $\pi/2$ for w=0 to a value $\Phi(\infty)<\pi$ and increasing with η. Thus, in contrast to the case of a perfectly conducting strip, the edge-on backscattering of a resistive strip tends to zero as $w\to 0$.

When the data for P^r are compared with the corresponding half plane currents at a distance w from the edge, it is found that

$$P^r(\pi,\pi) = i\alpha\{ZJ(w)\}^2 \tag{17}$$

with

$$\alpha \simeq 0.0313 + \eta 0.0663, \tag{18}$$

valid for $w \gtrsim \lambda/2$. The relation is directly analogous to (15) and reduces to it when $\eta=0$. It is therefore possible to deduce the front and rear edge contributions of strips from the half plane currents which are themselves given by (5).

5. Discussion

In seeking to select a strip resistance for low backscattering at edge-on incidence, we first note that if there were no limit to the resistances available the obvious choice would be $R/Z=\infty$, since then $J(x)=0$ and the strip no longer exists. In practice, of course, R is limited, and for the purposes of the following discussion it will be assumed that $R/Z \leq 5$, implying $\eta \leq 10$.

As indicated by (16), the scattering is the sum of front and rear edge contributions. From (9) and (11)

$$P^f(\pi,\pi) = -\frac{i\eta}{16}\{ZJ(0)\}^2 \tag{19}$$

and is minimized by choosing η as large as possible. Fig. 3 or, more directly, Fig. 1 of [1], then shows that, for $\eta=10$, $|P^f|$ is 26.6 dB below its value for a perfectly conducting strip. For very small strip widths, maximizing η also minimizes P^r, but for any given η there is a strip width beyond which P^r is least if $\eta=0$, i.e., if the rear edge is perfectly conducting. As seen from Fig. 9, when $\eta=10$ the transition occurs at $w\simeq 0.6\lambda$. This now suggests that for strips of larger width

the edge-on scattering would be a minimum if the resistance could be tapered from a maximum value at the front to zero at the rear in such a way as to avoid creation of new sources of scattering. With uniform strips, however, the best that can be done is to choose the maximum resistance available, and since the phasing between the front and rear edge contributions is virtually independent of η (see Fig. 8), this conclusion holds regardless of the strip width and apparently for complex η as well as real. If, therefore, the resistive strip were encased in, for example, fiberglas to provide rigidity, we could expect to observe the same effects apart from any changes due to differences in the real part of the resistance resulting from the presence of the fiberglas.

At aspects near broadside the backscattering cross section does not show the large variation as a function of w/λ characteristic of edge-on incidence, but the cross section reductions achieved when $\phi=\pi$ are at least indicative of the reduction at other aspects. This is evident from Fig. 10 where the backscattering cross sections of four different strips of width 1.25λ are plotted as functions of ϕ. When $\eta=4$, for example, the reduction exceeds 14 dB at all aspects compared with the 15.6 dB edge-on.

Acknowledgement

The author is indebted to Dr. V. V. Liepa and Mr. F. J. Samaha for assistance with the computations, and to the Air Force Office of Scientific Research for support under Grant 77-3188.

References

[1] T.B.A. Senior, "Half plane edge diffraction," Radio Sci., Vol. 10, pp. 645-650, June 1975.

[2] -----, "Diffraction by a semi-infinite metallic sheet," Proc. Roy. Soc. (London), Vol. 213A, pp. 436-458, 1952.

[3] A. T. Fialkovskiy, "Diffraction of planar electromagnetic waves by a slot and a strip," Radio Eng. Electron., Vol. 2, pp. 150-157, 1966.

[4] L. Peters, Jr., "End-fire echo area of long, thin bodies," IRE Trans. Antennas Propagat., Vol. AP-6, pp. 133-139, Jan. 1958.

Table 1. Deduced and Theoretical Front Edge Contributions $P^f(\pi,\pi)$

P^f / η	Deduced		Theor. = $-i\{K_+(k)\}^2/4$	
	modulus	phase (deg.)	modulus	phase (deg.)
1	0.1542	-90.4	0.1558	-90
2	0.0940	-90.4	0.0955	-90
4	0.0529	-90.3	0.0540	-90
6	0.0370	-90.2	0.0377	-90
10	0.0230	-90.0	0.0235	-90

Legends for Figures

Figure 1: Path of integration C in the complex ζ plane.

Figure 2: Strip geometry. For edge-on incidence, $\phi_o = \pi$.

Figure 3: Current at the edge of a resistive half plane as a function of η: ——— exact, ----- asymptotic (see 10).

Figure 4: Current amplitudes for five resistive half planes computed using strips 6λ wide, compared with the amplitude for a perfectly conducting half plane (-----).

Figure 5: Current amplitude computed (000) for a perfectly conducting strip 3λ wide compared with that for a half plane (———).

Figure 6: Backscattering cross section computed (000) for a perfectly conducting strip compared with the asymptotic approximation (13) (———).

Figure 7: Current amplitudes computed (000) for three resistive strips 3λ wide compared with those on the corresponding half planes (———).

Figure 8: Backscattering cross sections computed for three resistive strips.

Figure 9: Amplitudes of the rear edge contributions P^r for five resistive strips (———) compared with the contribution for perfectly conducting strips (-----) computed using (14). The crosses show the corresponding $|P^f|$ obtained from (11).

Figure 10: Backscattering cross section as a function of aspect from edge-on (ϕ=180°) to broadside (ϕ=90°) for four strips of width 1.25λ.

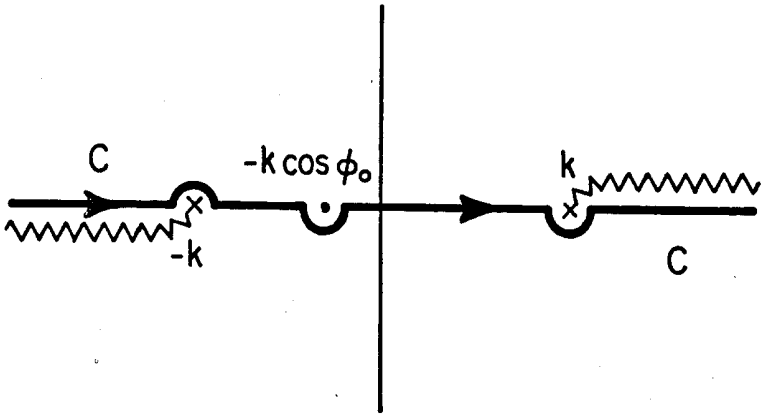

Figure 1

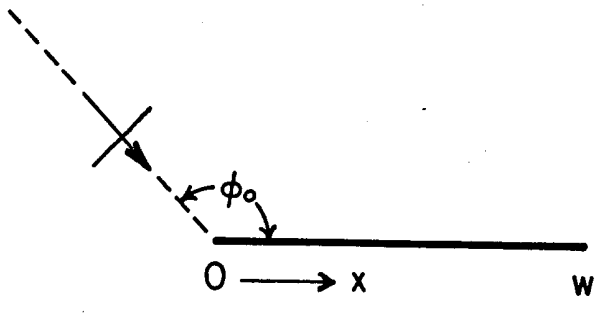

Figure 2

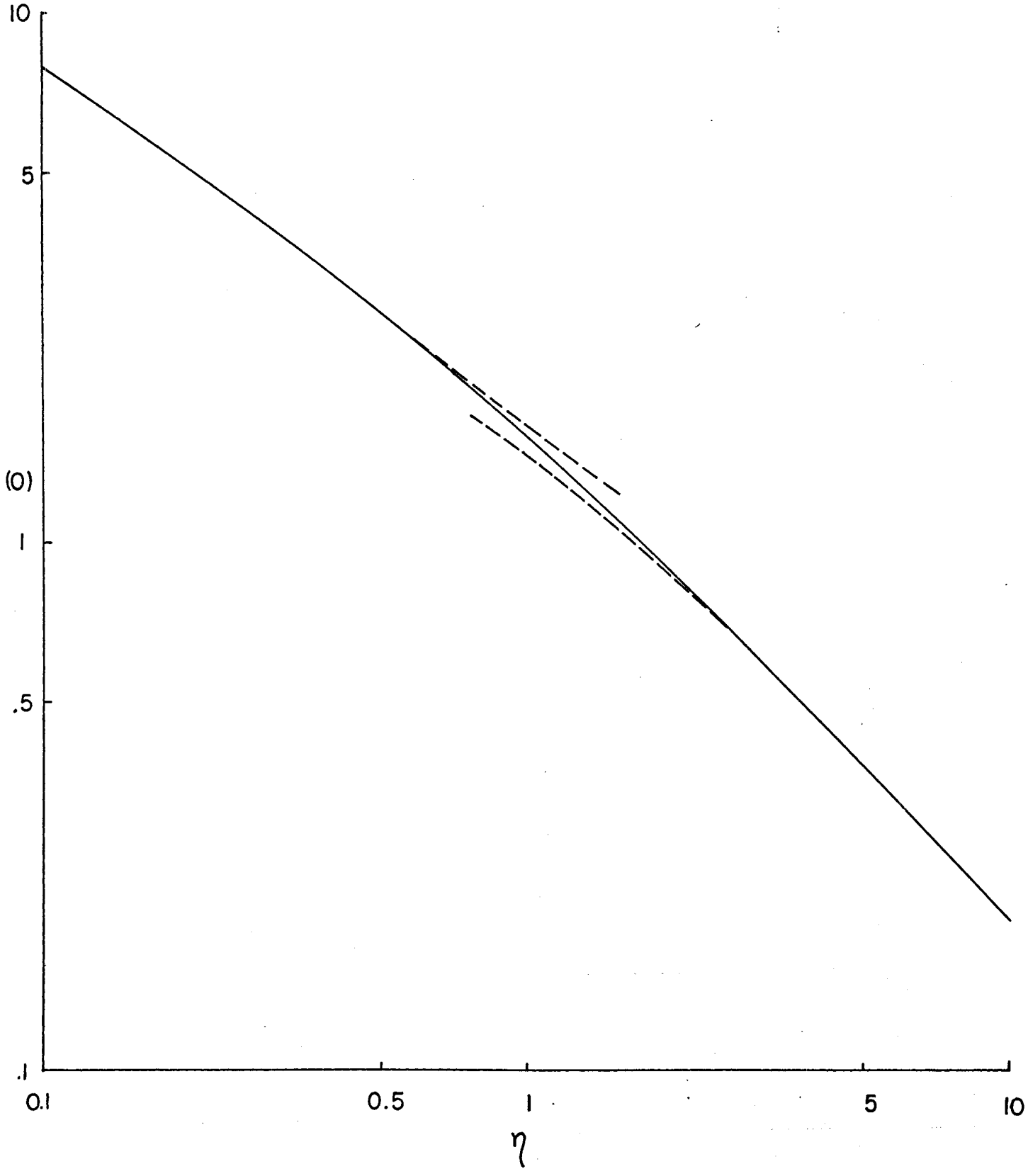

Figure 3

Figure 4

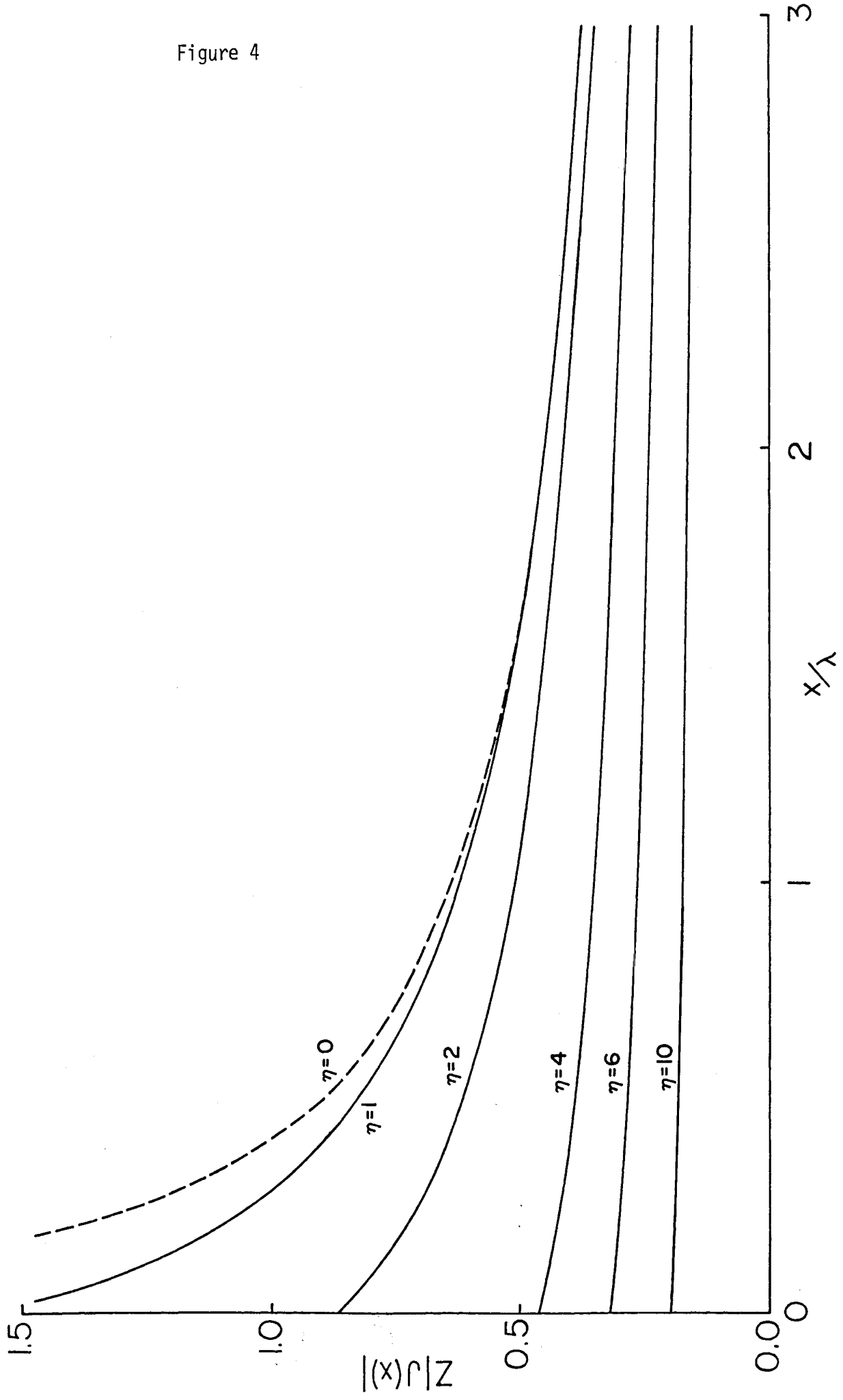

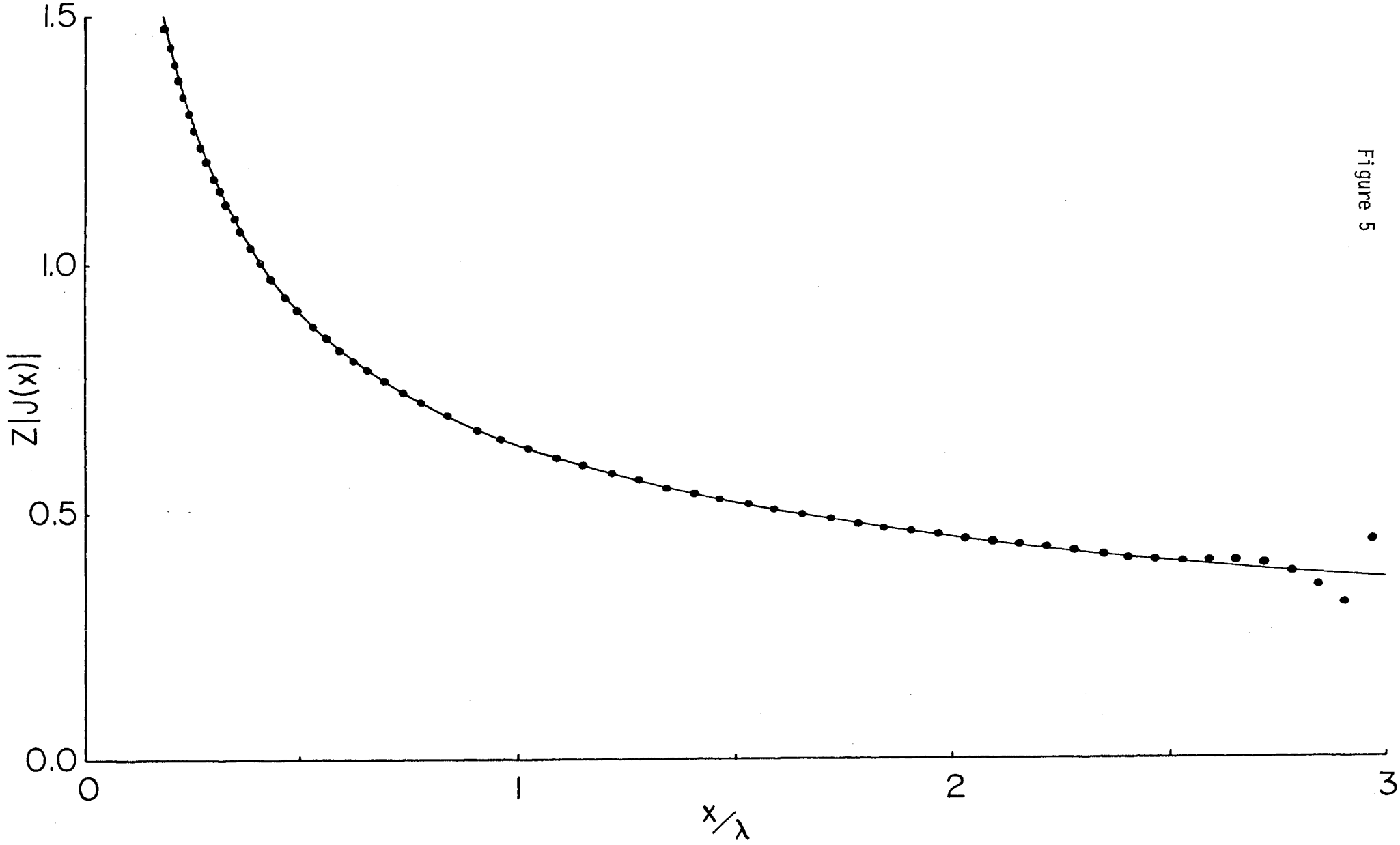

Figure 5

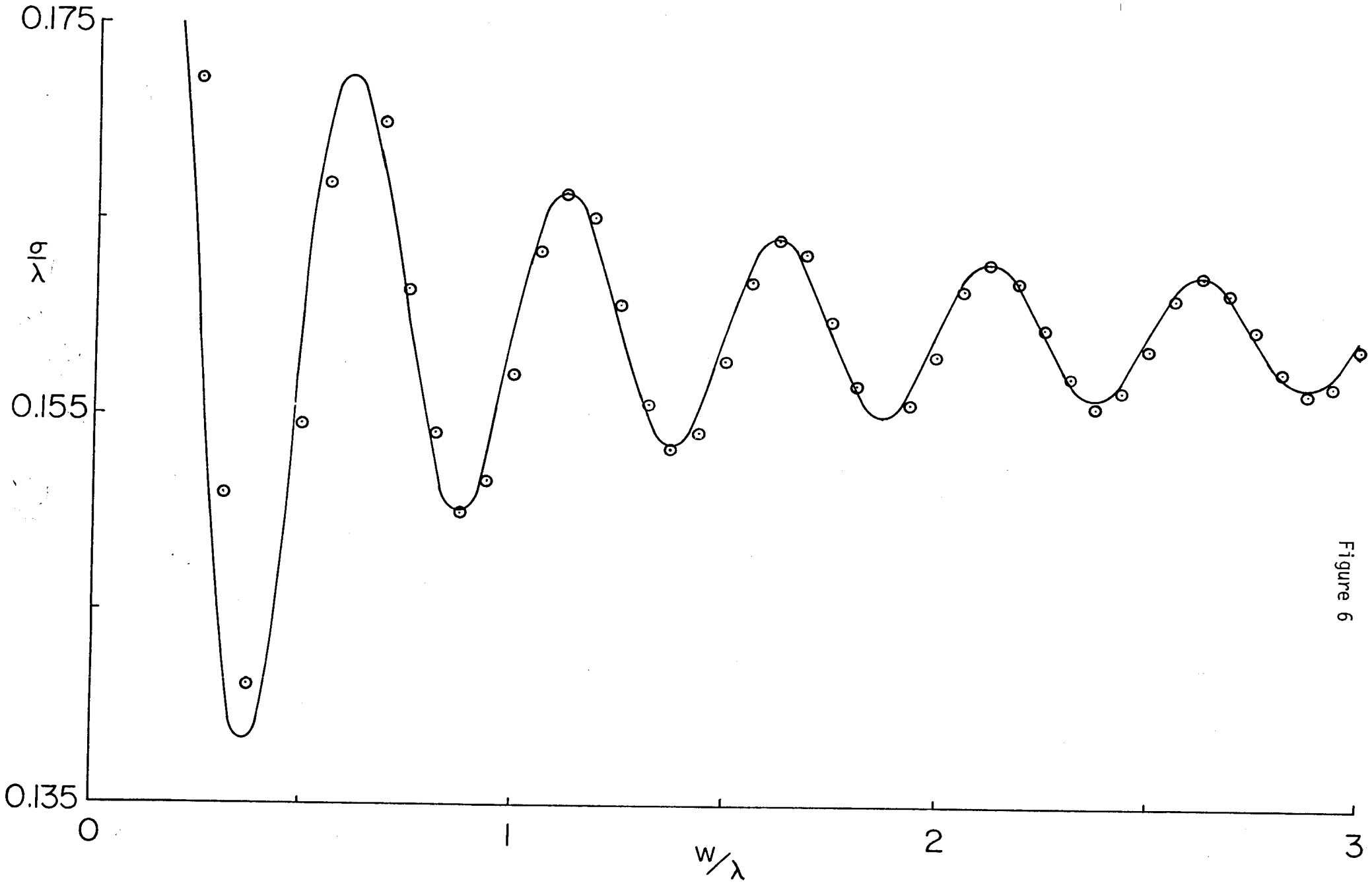

Figure 6

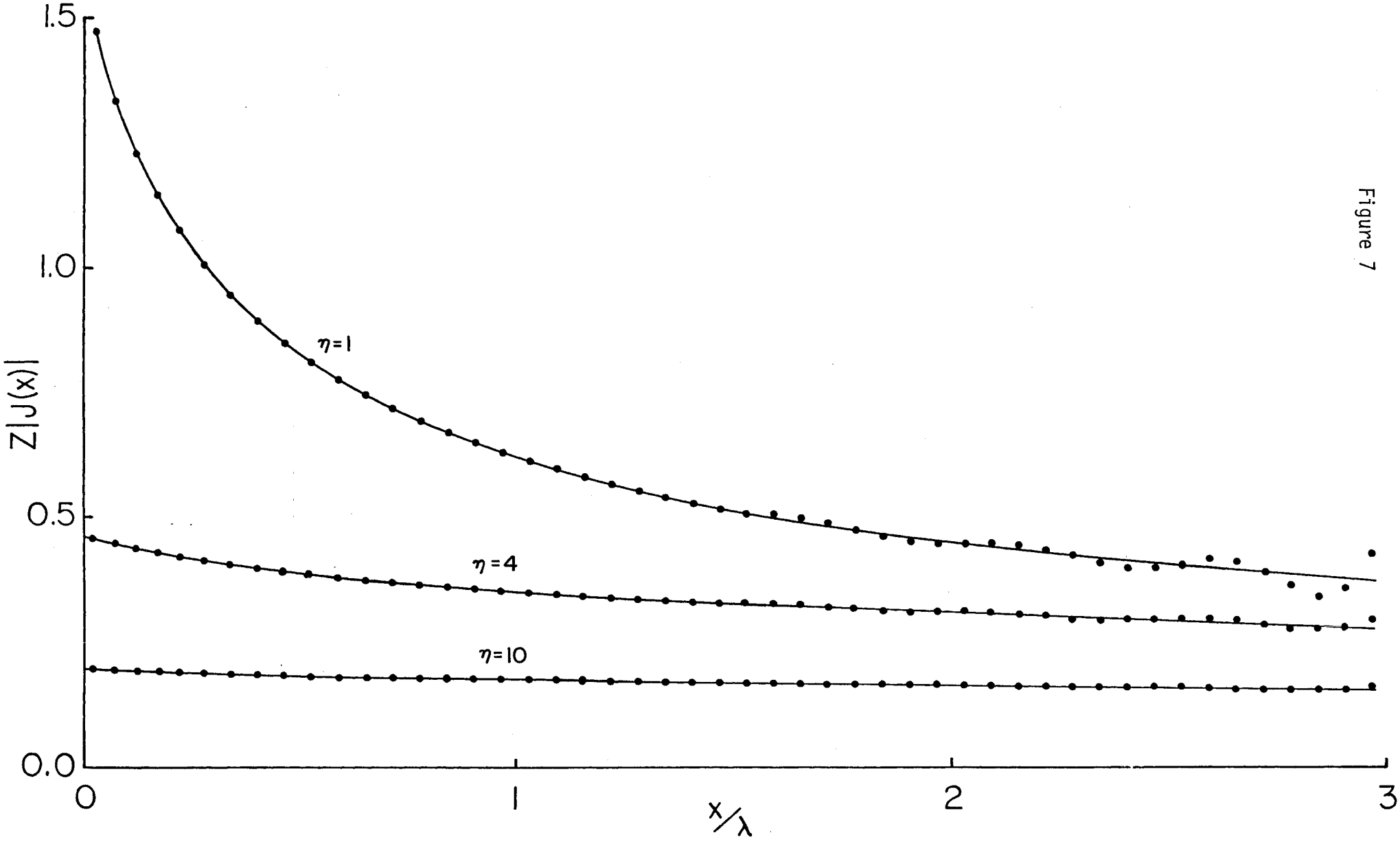

Figure 7

Figure 8

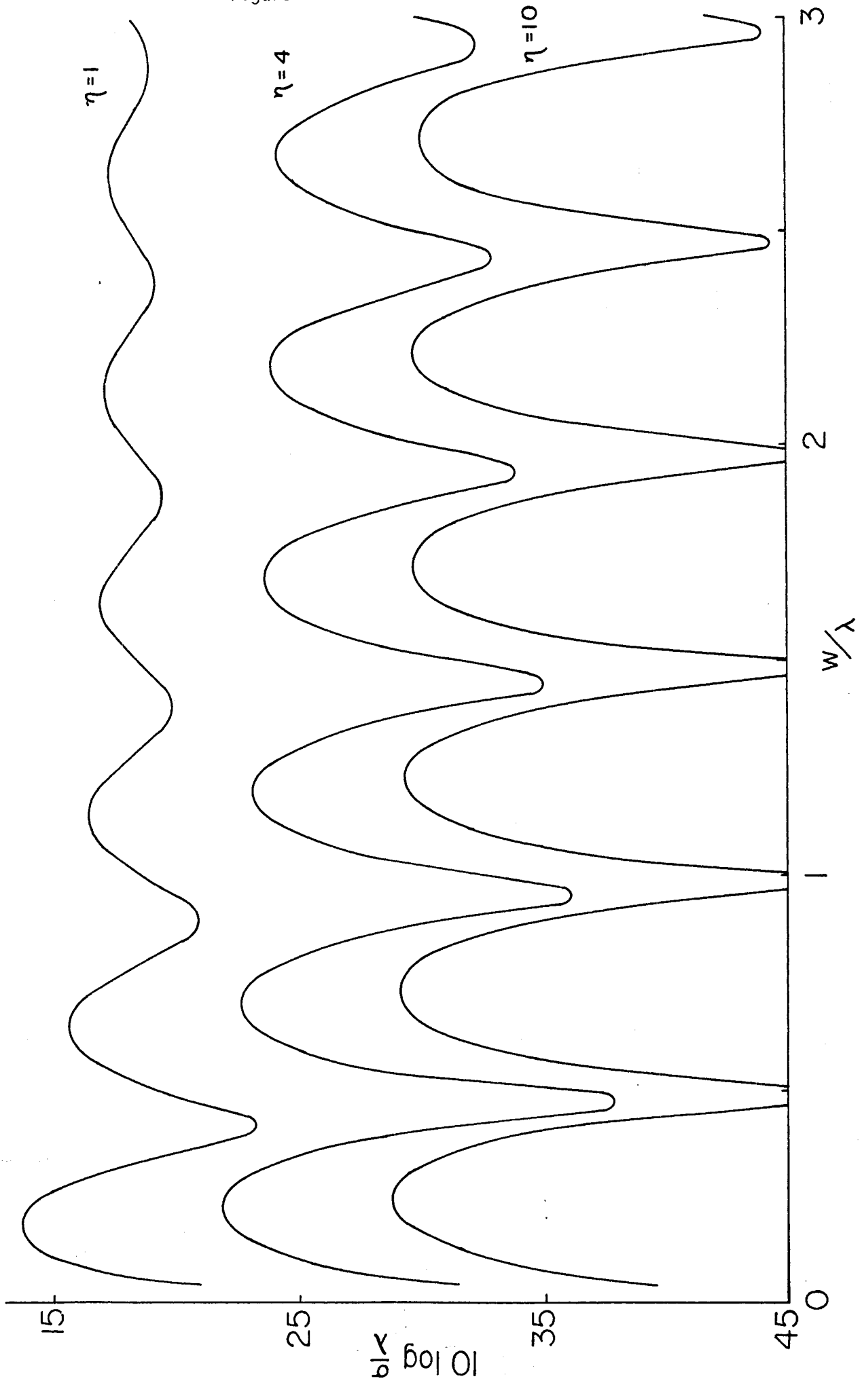

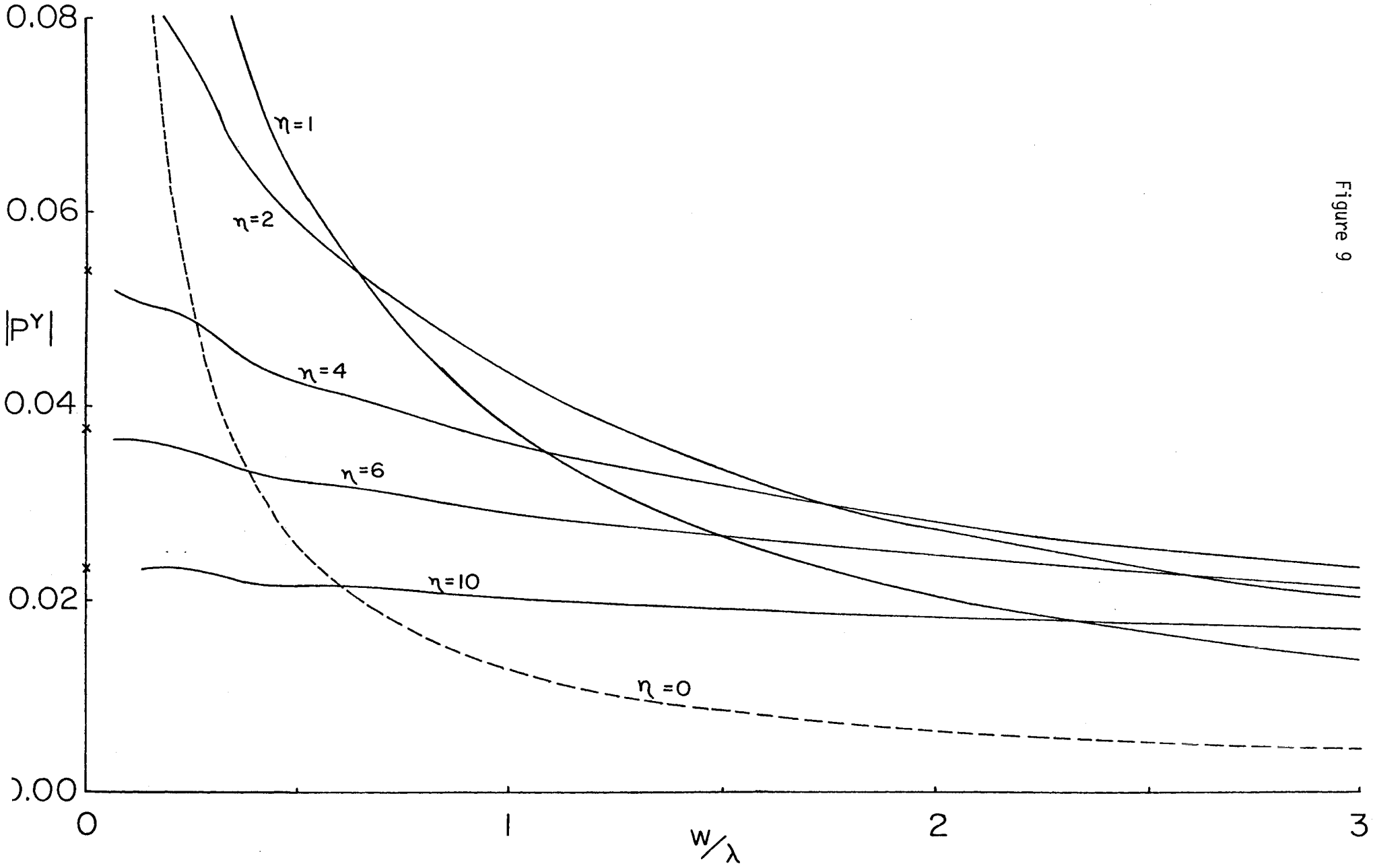

Figure 9

Figure 10